Adaptive Neuro-Fuzzy Optimization for Enhanced Precision in Laser Micro-Machining Operations

Sanjin Troha[1], Miloš Milovančević[2*], Aleksandar Dimov[3]

[1] Faculty of Engineering, University of Rijeka, 51000 Rijeka, Croatia
[2] Faculty of Mechanical Engineering, University of Niš, 18000 Niš, Serbia
[3] Faculty of Mathematics and Informatics (FMI), Sofia University, 1164 Sofia, Bulgaria

* Correspondence: Miloš Milovančević (milovancevic@masfak.ni.ac.rs)

Abstract: In this study, an intelligent optimization system for laser micro-machining operations is developed, utilizing an Adaptive Neuro-Fuzzy Inference System (ANFIS). The heuristic optimization tool, ANFIS, synergistically combines back-propagation training with gradient descent in a unidirectional manner. A comprehensive training set, incorporating experimental data from the literature, highlights the sensitivity of groove depth and recast layer height to specific critical operating factors during the laser micro-machining process. By optimizing lamp current, pulse width, and frequency, the proposed system aims to achieve superior groove depth and recast layer height outcomes. This novel microscopic research holds the potential to captivate both academic scholars and industry professionals.

Keywords: Laser micro-machining; Groove depth; Recast layer; Intelligent design; ANFIS

1 Introduction

Laser micro-machining offers the potential to enhance productivity by utilizing high energy density to create intricate shapes on various materials without inducing material stress or generating waste. This eco-friendly approach can significantly improve control, measurement, and assembly in the manufacturing of microproducts, where input quality management is of paramount importance.

Laser-electrochemical machining has been shown to produce material surfaces devoid of molten slag [1]. Additionally, water jet guided laser micro-machining, an innovative technique for hard brittle materials, has improved the cutting of mono-crystalline silicon [2]. Research indicates that reducing laser incidence angle can decrease micro-texture depth, laser machining temperature, and residual compressive stress [3], while micro-texture width and roughness are observed to increase concurrently.

Recent advancements, such as micro-injection molding, have successfully replicated microneedle cavities [4], while femtosecond laser cutting of battery separators and multi-pass groove machining on silicon have expanded the effective machining range and efficiency for both focused and defocused surfaces [5]. Nanoporous catalyst layers have enabled the surpassing of power density limitations [6], and CVD diamond-coated machines have produced composite microstructures at multiple scales [7]. Specific factors, including pulse duration of a few tens of picoseconds and laser pulse overlap rate, have been found to influence micro-machining of monocrystalline diamond using pulsed lasers [8]. The growing application of high-strength metals in micro-scale designs necessitates the development of superior micro-fabrication techniques [9].

This study aims to identify optimal input parameter selection methods for laser micro-machining through the implementation of the sophisticated Adaptive Neuro-Fuzzy Inference System (ANFIS) [10]. This system is designed to recognize and categorize operating parameters in the laser micro-machining process. The primary objective is to maximize groove depth while minimizing recast layer thickness. ANFIS exhibits effective data normalization and generalization capabilities, and is characterized by its resilience and fault tolerance. As a result, the ANFIS-based laser micro-machining process is expected to be highly adaptable to variations in a wide range of operating parameters [11–15].

In summary, this research seeks to advance laser micro-machining knowledge by investigating innovative optimization methods. This exploration aims to expedite the production of high-quality, miniaturized products with reduced resource consumption and environmental impact.

2 Methodology and Materials

2.1 Experimental Setup

The experimental procedure utilized a Nd:YAG computer numerically controlled pulsed laser machining system. This apparatus generated a 1 mm-diameter laser beam with a 100 µm spot size. Input values were systematically adjusted in each cycle. Laser operations etched the sample surface. Table 1 presents the input or operating parameters and silver nanoparticle sizes, as reported in the study [11].

V-groove depth was employed as a measure of surface etching. Each activity aimed to optimize or reduce groove depth. For optimal surface quality, the recast layer height should be minimized. Table 1 displays the input and output parameters used in this study, based on the study [11]. The input parameters included lamp current, pulse rate, pulse width, and ambient pressure. All possible combinations of these parameters at various levels were examined.

Table 1. Input and output variables [11]

Inputs				Outputs	
Lamp current	Pulse frequency	Pulse width	Air pressure	Depth of groove (mm)	Height of recast layer (mm)
0.87799	0.59987	0.49	0.49	0.099265	0.099385
0.87799	0.499987	0.49	0.99	0.0993175	0.09938375
0.87799	0.499987	0.99	0.49	0.099215	0.09938125
0.87799	0.499987	0.99	0.99	0.099265	0.09933375
0.87799	0.7998	0.75	0.75	0.099278	0.09943
0.87799	0.99	0.49	0.49	0.0992175	0.09922875
0.87799	0.99	0.49	0.99	0.09924	0.09929375
0.87799	0.99	0.99	0.49	0.09916	0.0992875
0.87799	0.99	0.99	0.99	0.0992325	0.0992837
0.9399	0.499977	0.75	0.99	0.09923	0.099168
0.9399	0.7998	0.75	0.75	0.0992646	0.0992928
0.9399	0.7998	1	0.49	0.0992866	0.099523
0.9399	1	0.49	0.75	0.0992217	0.099188
0.99	0.499977	0.49	0.49	0.099345	0.0994825
0.99	0.499987	0.49	0.99	0.09935	0.0994075
0.99	0.499987	0.99	0.49	0.09932	0.09949125
0.99	0.499987	0.99	0.75	0.099268	0.099413
0.99	0.499987	0.99	0.99	0.09934	0.09941875
0.99	0.7998	0.49	0.99	0.099376	0.09944
0.99	0.99	0.49	0.49	0.0993075	0.0993475
0.99	0.99	0.49	0.99	0.0993125	0.09936125
0.99	0.99	0.75	0.49	0.099308	0.099598
0.99	0.99	0.99	0.49	0.09927	0.09938375
0.99	0.99	0.99	0.99	0.09932	0.09927375

2.2 ANFIS Methodology

Figure 1 illustrates the five layers of the ANFIS architecture. The ANFIS network is driven by fuzzy inference. In the first layer, membership functions convert input parameters into fuzzy values. For this study, the bell-shaped membership function was employed due to its superior nonlinear data regression capabilities.

The bell-shaped membership function is defined as follows:

$$\mu(x) = \text{bell}\,(x; a_i; b_i; c_i) = \frac{1}{1 + \left[\left(\frac{x - c_i}{a_i}\right)^2\right]^{b_i}} \tag{1}$$

where, $\{a_i, b_i, c_i\}$ represents the parameter set and x input.

Layer 2 of the ANFIS architecture multiplies the fuzzy signals obtained from Layer 1 to determine each rule's firing strength. In Layer 3, known as the rule layer, the signals from Layer 2 are normalized. Layer 4 is responsible for defuzzifying the signals and inferring rules. Finally, Layer 5 aggregates all the inputs to produce the output.

This study introduces a novel experimental setup and the sophisticated ANFIS approach to enhance laser micro-machining performance. By optimizing the configuration to maximize groove depth and minimize recast layer height, this method aims to achieve high-quality surface finishes.

Layer 1 Input layer	→	Layer 2 Multiplies fuzzy signals	→	Layer 3 Rule layer	→	Layer 4 Inference of rules	→	Layer 5 Output layer

Figure 1. ANFIS layers

3 Results and Discussion

The ANFIS approach successfully identified crucial predictors for fault types. This method streamlined the analysis by selecting and preparing relevant input parameters, eliminating unnecessary data. As demonstrated below, the dataset was divided into a training set (odd-indexed samples) and a testing set (even-indexed samples) using MATLAB software.

```
»[data] = depth;
»trn_data = data(1:2:end,:);
»chk_data = data(2:2:end,:);
»[data] = height;
»trn_data = data(1:2:end,:);
»chk_data = data(2:2:end,:);
```

Exhaustive searches were conducted using the "exhsrch" function to determine the inputs that had the most significant impact on groove depth and recast layer height. The first parameter of the function represents the number of input permutations. For each permutation, "exhsrch" generates an ANFIS model, trains it for one epoch, and records the results. The top two predictors for outcomes were identified using the following command line:

```
» exhsrch(1,trn_data,chk_data);
» exhsrch(2,trn_data,chk_data);
```

Table 2 and Table 3 present the relationships between groove depth and single input, as well as recast layer height. These parameters were ascertained based on the training (trn) and checking (chk) root-mean-squared error (RMSE). Lamp current, which exhibited the lowest training error, had the most significant influence on both groove depth and recast layer height. Consequently, minor changes in lamp current may affect these two parameters.

As shown in Table 2, the combination of lamp current and pulse width yielded the largest impact on groove depth, as it reduced the training error. In contrast, Table 3 reveals that a combination of lamp current and pulse frequency had the most substantial effect on the final recast layer height, resulting in the lowest training error.

Based on the various input combinations, Figure 2 and Figure 3 depict the ANFIS decision surfaces for groove depth and recast layer height, respectively.
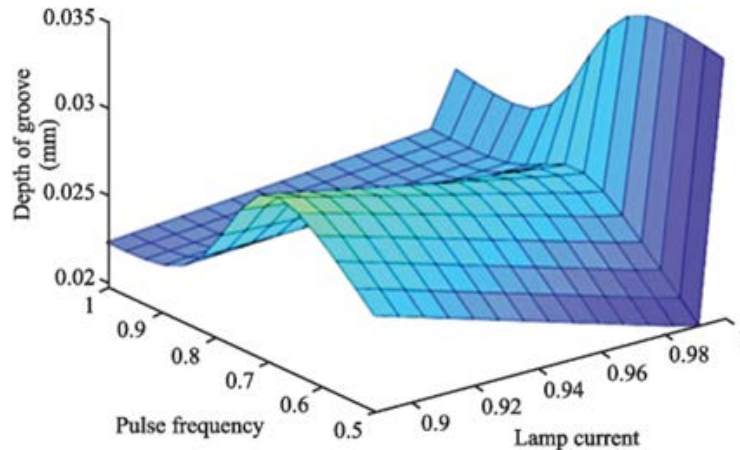

Figure 2. ANFIS decision surface for depth of groove based on two selected parameters
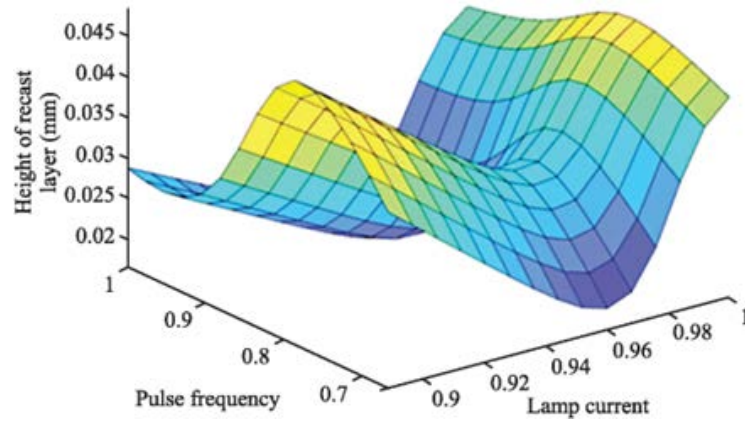
Figure 3. ANFIS decision surface for height of recast layer based on two selected parameters

Table 2. Correlations of one and two attributes with depth of groove

Lamp current	trn = 0.099032, chk = 0.099038			
Lamp current	trn = 0.099032,			
	chk = 0.099038			
Pulse frequency	trn = 0.099021,	trn = 0.099043,		
	chk = 0.099039	chk = 0.099055		
Pulse width	trn = 0.099014,	tr = 0.099029,	trn = 0.099042,	
	chk = 0.099048	chk = 0.099059	chk = 0.099059	
Air pressure	trn = 0.099019,	trn = 0.099021,	trn = 0.099032,	trn = 0.099041,
	chk = 0.099051	chk = 0.099073	chk = 0.099064	chk = 0.099057

Table 3. Correlations of one and two attributes with height of recast layer

Lamp current	trn = 0.099046,		
	chk = 0.099122		
Pulse frequency	trn = 0.099005,	trn = 0.099056,	
	chk = 0.099108	chk = 0.099125	
Pulse width	trn = 0.099032,	trn = 0.099050,	trn = 0.099071,
	chk = 0.099113	chk = 0.099123	chk = 0.099125
Air pressure	trn = 0.099027,	trn = 0.099033,	trn = 0.099042,	trn = 0.099069,
	chk = 0.099138	chk = 0.099121	chk = 0.099110	chk = 0.099119

4 Conclusions

In this study, the influence of operational parameters on groove depth and recast layer height during laser micro-machining was investigated using experimental training data from the literature. Achieving optimal results in laser micro-machining necessitates the adjustment of groove depth and recast layer height.

The findings reveal that lamp current and pulse width significantly impact groove depth. These factors may substantially alter groove depth during laser micro-machining, indicating that adjusting these parameters can help attain maximum groove depth. Additionally, the recast layer height was found to be most responsive to lamp current and pulse frequency. This observation suggests that optimizing these settings may aid in achieving the desired shallow recast layer depth.

This preliminary study provides valuable insights into the complex relationships between operational factors and machining outcomes during laser micro-machining, offering guidance for researchers and practitioners in the field.

As shown in Table 2 and Table 3, the root-mean-squared training (trn) and checking (chk) errors were employed to ascertain the effects of single and double input combinations on groove depth and recast layer height. Lamp current was found to have the most significant influence on both parameters, according to the minimal training error. Consequently, minor variations in lamp current may lead to considerable changes in these two parameters.

The Adaptive Neuro-Fuzzy Inference System (ANFIS) is a hybrid computational model that combines fuzzy logic and neural network techniques to provide normalization, generalization, noise resistance, and fault tolerance. This model excels at handling complex, nonlinear data relationships. In laser micro-machining, ANFIS is utilized to model and predict the relationships between input (lamp current, pulse width, pulse frequency) and output (groove depth, recast layer height) parameters. The technique leverages ANFIS's inherent ability to learn from experimental training data samples, generating a fuzzy inference system that captures data patterns and correlations.

Once trained, the ANFIS model can make predictions under various conditions, including changes in operational parameters. The robust normalization and generalization capabilities of ANFIS ensure that predictions for laser micro-machining remain accurate despite alterations in operational parameters. To validate that the ANFIS model accurately represents the laser micro-machining process under varying operational conditions, sensitivity tests and experimental data should be employed. In cases where new information or significant changes in operational parameters or systems arise, the ANFIS model may require updates.

This study sheds light on the intricate relationships between various operational aspects in laser micro-machining, introducing new optimization and predictive modeling approaches. Future research could leverage the predictive power of ANFIS to investigate additional operational factors and their relationships, further enhancing laser micro-machining operations.

Data Availability

The data used to support the findings of this study are available from the corresponding author upon request

Conflicts of Interest

The authors declare no conflict of interest.

References

[1] A. Sun, Y. B. Chang, and H. J. Liu, "Metal micro-hole formation without recast layer by laser machining and electrochemical machining," *Optik*, vol. 171, pp. 694–705, 2018. https://doi.org/10.1016/j.ijleo.2018.06.099

[2] H. C. Qiao, Z. F. Cao, J. F. Cui, and J. B. Zhao, "Experimental study on water jet guided laser micro-machining of mono-crystalline silicon," *Opt. Laser Technol.*, vol. 140, p. 107057, 2021. https://doi.org/10.1016/j.optlastec.2021.107057

[3] Y. Lu, J. X. Deng, R. Wang, J. X. Wu, and Y. Meng, "Tribological performance of micro textured surface machined by Nd: YAG laser with different incident angle," *Opt. Laser Technol.*, vol. 148, p. 107768, 2022. https://doi.org/10.1016/j.optlastec.2021.107768

[4] M. Gülçür, J. M. Romano, P. Penchev, T. Gough, E. Brown, S. Dimov, and B. Whiteside, "A cost-effective process chain for thermoplastic microneedle manufacture combining laser micro-machining and micro-injection moulding," *CIRP J. Manuf. Sci. Technol.*, vol. 32, pp. 311–321, 2021. https://doi.org/10.1016/j.cirpj.2021.01.015

[5] X. J. Du, S. Kang, and C. B. Arnold, "Optimization of ultrafast axial scanning parameters for efficient pulsed laser micro-machining," *J. Mater. Process. Technol.*, vol. 288, p. 116850, 2021. https://doi.org/10.1016/j.jmatprotec.2020.116850

[6] J. Iglesia, C. C. Lang, Y. M. Chen, S. Y. Chen, and C. J. Tseng, "Raising the maximum power density of nanoporous catalyst film-based polymer-electrolyte-membrane fuel cells by laser micro-machining of the gas diffusion layer," *J. Power Sources*, vol. 436, p. 226886, 2019. https://doi.org/10.1016/j.jpowsour.2019.226886

[7] B. Guo, J. Zhang, M. Wu, Q. Zhao, H. Liu, A. Monier, and J. Wang, "Water assisted pulsed laser machining of micro-structured surface on CVD diamond coating tools," *J. Manuf. Process.*, vol. 56, pp. 591–601, 2020. https://doi.org/10.1016/j.jmapro.2020.04.066

[8] Y. Okamoto, A. Okada, A. Kajitani, and T. Shinonaga, "High surface quality micro machining of monocrystalline diamond by picosecond pulsed laser," *CIRP Annals*, vol. 68, no. 1, pp. 197–200, 2019. https://doi.org/10.1016/j.cirp.2019.04.119

[9] S. Bhandari, M. Murnal, J. Cao, and K. Ehmann, "Comparative experimental investigation of micro-channel fabrication in Ti alloys by laser ablation and laser-induced plasma micro-machining," *Proc. Manuf.*, vol. 34, pp. 418–423, 2019. https://doi.org/10.1016/j.promfg.2019.06.186

[10] J. S. R. Jang, "ANFIS: Adaptive-network-based fuzzy inference systems," *IEEE Trans. Syst. Man Cybern.*, vol. 23, no. 3, pp. 665–685, 1993. https://doi.org/10.1109/21.256541

[11] S. K. Dhara, A. S. Kuar, and S. Mitra, "An artificial neural network approach on parametric optimization of laser micro-machining of die-steel," *Int. J. Adv. Manuf. Technol.*, vol. 39, no. 1, pp. 39–46, 2008. https://doi.org/10.1007/s00170-007-1199-1

[12] D. N. Sharma and J. R. Kumar, "Optimization of dross formation rate in plasma arc cutting process by response surface method," *Mater. Today Proc.*, vol. 32, pp. 354–357, 2020. https://doi.org/10.1016/j.matpr.2020.01.605

[13] A. Rajeshkannan, M. Ali, R. Prakash, R. Prasad, A. K. Jeevanantham, and K. M. Jayaram, "Optimizing the process parameters in plasma arc cutting using Taguchi approach for the case industry in Fiji," *Mater. Today Proc.*, vol. 24, pp. 1122–1131, 2020. https://doi.org/10.1016/j.matpr.2020.04.425

[14] D. Singh and Y. Shrivastava, "Identification of suitable machining zone during the plasma arc cutting of SS-304," *Mater. Today Proc.*, vol. 38, pp. 413–417, 2021. https://doi.org/10.1016/j.matpr.2020.07.598

[15] A. Suresh and G. Diwakar, "Optimization of process parameters in plasma arc cutting for TWIP steel plates," *Mater. Today Proc.*, vol. 38, pp. 2417–2424, 2021. https://doi.org/10.1016/j.matpr.2020.07.383